Automatically Tunable AMF for Radar Detection in Diffuse Multipath

Yao Rong
College of Math. and Statist.
Yunnan University
Kunming, Yunnan 650091, China
rongyao0618@outlook.com

Augusto Aubry, Antonio De Maio
DIETI
University of Naples "Federico II"
80125 Naples, Italy
augusto.aubry@unina.it; ademaio@unina.it

Mengjiao Tang
Center for Inf. Eng. Science Research
Xi'an Jiaotong University
Xi'an, Shaanxi 710049, China
qingqing_tmj@126.com

***Abstract*—This paper studies adaptive radar detection of point-like targets in the presence of Gaussian interference and possible diffuse multipath. For this problem, a Tunable Adaptive Matched Filter (T-AMF) detector which contains a tuning parameter ruled by the strength of multipath effects was proposed. This paper develops a two-stage strategy for the selection of the tuning parameter by jointly using a two-step energy detector and the expected likelihood (EL)-based principle. Once plugged into the T-AMF, the selected parameter yields a fully adaptive detector free of any user parameter. Remarkably, the new architecture possesses the desired constant false alarm rate (CFAR) property with respect to the disturbance covariance. Finally, its detection performance is assessed and validated via numerical examples.**

***Index Terms*—Diffuse multipath, adaptive signal detection, tuning parameter, energy detector, expected likelihood approach.**

I. Introduction

TARGET detection in diffuse multipath environments is a challenging research topic in radar signal processing. When multipath occurs, the radar site receives the signal backscattered from the target via many propagation paths including a direct path and some indirect paths [1]. The indirect paths usually arise when waves are reflected by rough or glistening surfaces [1]–[4]. Therefore, the useful target returns contain not only the backscattered line-of-sight component but also indirect-path contributions. In practical scenarios, the combination of multipath waves is highly sensitive to the number of paths, directions of arrival, strength of echoes, and Doppler shifts [1], which are usually not predictable because of unknown "space-time-varying" reflection characteristics of the surrounding glistening surface [4]. As a result, the diffuse multipath can cause a mismatch of the line-of-sight target signature in the cell under test, and conventional adaptive strategies [5]–[9] are no longer able to provide a reliable detection.

Many works have devoted to overcoming the influence of the multipath effects on radar signal processing. Several knowledge-aided adaptive detection approaches have been developed by leveraging prior knowledge of the radar-target environment [10] and the reflected steering vector [11], [12]. When the mismatched steering vector belongs to a given signal subspace, some robust subspace detectors have been provided in [13]–[21]. Based on the constrained generalized likelihood ratio (GLR) criterion, the Conic Acceptance Detector (CAD) [22], [23], the robust Adaptive Matched Filter (AMF) [24], and the Tunable AMF (T-AMF) [4], which are all tunable detectors, have been proposed to improve the performance of the conventional GLR test. Unfortunately, the involved tuning parameters can be hardly set in time-varying scenarios, and a poor selection may lead to performance degradations.

In this paper, adaptive detection of point-like targets in the presence of Gaussian interference and possible diffuse multipath is investigated, and an innovative two-stage approach is proposed to determine the tuning parameter in the T-AMF. The first stage determines the presence or absence of multipath effects via a covariance matrix equality testing (resorting to a two-step energy detector (ED)); the second stage provides an estimation of the tuning parameter (according to an expected likelihood (EL)-based approach [25]–[28]) when the hypothesis of multipath presence is accepted. Combining the T-AMF with the two-stage selection procedure leads to a fully adaptive detector that is free of any user parameter. This design scheme also applies to adaptive detection of range-distributed targets, which is studied in our another paper [29]. Remarkably, the new adaptive detector ensures the constant false alarm rate (CFAR) property. Finally, we conduct numerical examples to assess the detection capabilities.

The remainder of this paper is organized as follows. Section

Notations—Throughout this paper, scalars are denoted by regular letters, vectors and matrices by boldface lowercase and uppercase letters, respectively. $\mathbb{C}^M$ is the set of M-dimensional complex column vectors. $\mathbb{C}^{M\times N}$ is the set of $M \times N$ complex matrices. For a complex number x, $|x|$ represents the modulus of x. The Euclidean norm of a vector $\boldsymbol{b}$ is denoted by $\|\boldsymbol{b}\|$. Symbols $(\cdot)^{\mathrm{T}}$ and $(\cdot)^{\dagger}$ stand for transpose and conjugate transpose, respectively. We denote by $\boldsymbol{I}_N$ the $N\times N$ identity matrix and by $\mathbf{0}$ the null vector or matrix of a proper dimension. For a matrix $\boldsymbol{A}$, $\|\boldsymbol{A}\|_2$ and $\det(\boldsymbol{A})$ denote its spectral norm and its determinant, respectively. $\mathrm{Diag}(\cdot)$ denotes a diagonal matrix formed from its vector argument. The curled inequality symbol $\succeq$ (and its strict form $\succ$) is used to denote generalized matrix inequality: for any $\boldsymbol{A} \in \mathbb{C}^{N\times N}$, $\boldsymbol{A} \succeq \mathbf{0}$ means that $\boldsymbol{A}$ is a positive semi-definite matrix ($\boldsymbol{A} \succ \mathbf{0}$ for positive definiteness). $\boldsymbol{A} \otimes \boldsymbol{B}$ indicates the Kronecker product of matrices $\boldsymbol{A}$ and $\boldsymbol{B}$. Finally, $\boldsymbol{X} \sim \mathcal{CN}_{N,M}(\boldsymbol{B}, \boldsymbol{C}, \boldsymbol{D})$ denotes a complex circular Gaussian distributed matrix $\boldsymbol{X} \in \mathbb{C}^{N\times M}$ with mean matrix $\boldsymbol{B}$ and covariance matrix $\boldsymbol{C} \otimes \boldsymbol{D}$ (i.e., the covariance matrix of $\mathrm{vec}(\boldsymbol{X})$), where $\boldsymbol{B} \in \mathbb{C}^{N\times M}$, $\boldsymbol{C} \in \mathbb{C}^{M\times M}$, and $\boldsymbol{D} \in \mathbb{C}^{N\times N}$.

This work was supported in part by the University of Naples "Federico II", and the National Natural Science Foundation of China under Grant 61903295.
(Corresponding author: Mengjiao Tang)

II formulates the problem and introduces the T-AMF. Section III focuses on the design of an adaptive selection procedure for the tuning parameter. Section IV provides some case studies to assess the effectiveness of the considered detectors. Section V contains conclusions.

II. Problem Formulation

Assume that a radar collects data from N (temporal, spatial, or spatial-temporal) channels. Let $\overline{\boldsymbol{z}} \in \mathbb{C}^N$ be a vector of the data under test (primary data) including possible target returns and disturbance, and suppose the availability of training data (secondary data) $\overline{\boldsymbol{y}}_1, \ldots, \overline{\boldsymbol{y}}_K \in \mathbb{C}^N$, free of useful signal. Let us focus on the detection of point-like targets in the presence of a possible diffuse multipath signal produced by a glistening or rough surface, where the direct-path signal is associated with the known target steering vector $\boldsymbol{p} \in \mathbb{C}^N$. In this scenario, the signal backscattered from the target is received via multiple propagation paths. Let $\boldsymbol{Q}$ be a unitary matrix with its first row equal to $\frac{\boldsymbol{p}^\dagger}{\|\boldsymbol{p}\|}$. After rotating the observation data by $\boldsymbol{Q}$: $\boldsymbol{z} = \boldsymbol{Q}\overline{\boldsymbol{z}}, \boldsymbol{y}_k = \boldsymbol{Q}\overline{\boldsymbol{y}}_k, k = 1, \ldots, K$, the problem under consideration can be formulated as a binary hypothesis test with the following canonical form:

$$\begin{cases} \mathcal{H}_0 : \begin{cases} \boldsymbol{z} = \boldsymbol{n}, \\ \boldsymbol{y}_k = \boldsymbol{n}_k, \ k = 1, \ldots K, \end{cases} \\ \mathcal{H}_1 : \begin{cases} \boldsymbol{z} = \alpha \boldsymbol{e}_1 + \boldsymbol{s} + \boldsymbol{n}, \\ \boldsymbol{y}_k = \boldsymbol{n}_k, \ k = 1, \ldots K, \end{cases} \end{cases} \tag{1}$$

where

- $\boldsymbol{e}_1 = [1, 0, \ldots, 0]^{\mathrm{T}}$ is the N-dimensional canonical-form target steering vector associated with the direct path;
- $\alpha \in \mathbb{C}$ denotes the (unknown) deterministic amplitude parameter, accounting for both target reflectivity and propagation effects on the direct path;
- $\boldsymbol{n}$ and $\boldsymbol{n}_k$'s are disturbance vectors, and $[\boldsymbol{n}, \boldsymbol{n}_1, \ldots, \boldsymbol{n}_K] \sim \mathcal{CN}_{N,K+1}(\boldsymbol{0}, \boldsymbol{I}_{K+1}, \boldsymbol{M})$ with $\boldsymbol{M} \succ \boldsymbol{0}$ and $K \geq N$;
- $\boldsymbol{s} \in \mathbb{C}^N$ represents the vector of echoes from indirect paths due to diffuse multipath phenomena, which is assumed to follow a zero-mean complex circular Gaussian distribution, i.e., $\boldsymbol{s} \sim \mathcal{CN}_N(\boldsymbol{0}, \boldsymbol{\Sigma})$, with unknown $\boldsymbol{\Sigma} \succeq \boldsymbol{0}$.

Define $\boldsymbol{R} \triangleq \boldsymbol{M} + \boldsymbol{\Sigma}$. The probability density function (pdf) of the primary data under $\mathcal{H}_1$ is given by

$$p_1(\boldsymbol{z}; \alpha, \boldsymbol{R}) = \frac{1}{\pi^N \det(\boldsymbol{R})} \exp\left[-(\boldsymbol{z} - \alpha\boldsymbol{e}_1)^\dagger \boldsymbol{R}^{-1} (\boldsymbol{z} - \alpha\boldsymbol{e}_1)\right],$$

and under $\mathcal{H}_0$, its pdf is given by letting $\alpha = 0$ and $\boldsymbol{R} = \boldsymbol{M}$. For the detection problem (1), the decision statistic of the T-AMF proposed by [4] can be written as

$$T_{\text{T-AMF}}(\varepsilon) = \frac{\max\limits_{\alpha \in \mathbb{C}, \boldsymbol{R} \in \Omega_\varepsilon} p_1(\boldsymbol{z}; \alpha, \boldsymbol{R})}{p_0(\boldsymbol{z}; \widehat{\boldsymbol{M}})} \tag{2}$$

$$= (1+\varepsilon)^{(N-1)} \frac{\widehat{\lambda}(\varepsilon) \exp(\boldsymbol{z}^\dagger \widehat{\boldsymbol{M}}^{-1} \boldsymbol{z})}{\exp\left(\widehat{\lambda}(\varepsilon)\widehat{\omega}\right)}, \tag{3}$$

where

- $\widehat{\boldsymbol{M}}$ is a consistent estimate of $\boldsymbol{M}$ defined by

$$\widehat{\boldsymbol{M}} = \frac{1}{K} \sum_{k=1}^{K} \boldsymbol{y}_k \boldsymbol{y}_k^\dagger = \begin{bmatrix} \widehat{m}_{11} & \widehat{\boldsymbol{m}}_{21}^\dagger \\ \widehat{\boldsymbol{m}}_{21} & \widehat{\boldsymbol{M}}_{22} \end{bmatrix} \in \mathbb{C}^{N \times N}, \tag{4}$$

  with $\widehat{\boldsymbol{m}}_{21} \in \mathbb{C}^{N-1}$, $\widehat{\boldsymbol{M}}_{22} \in \mathbb{C}^{(N-1)\times(N-1)}$, and $\widehat{m}_{11} > 0$ (with probability 1);
- $\Omega_\varepsilon = \{\boldsymbol{R} \succ \boldsymbol{0} : \|\boldsymbol{I}_N - \widehat{\boldsymbol{M}}^{\frac{1}{2}} \boldsymbol{R}^{-1} \widehat{\boldsymbol{M}}^{\frac{1}{2}}\|_2 \leq \varepsilon\}$ with $\varepsilon \geq 0$ defining a neighborhood of $\boldsymbol{R}$ whose "quasi-whitened" inverse $\widehat{\boldsymbol{M}}^{\frac{1}{2}} \boldsymbol{R}^{-1} \widehat{\boldsymbol{M}}^{\frac{1}{2}}$ is ε-similar to the identity matrix in terms of the spectral norm;
- $\boldsymbol{z} = [z_1, \boldsymbol{z}_2^{\mathrm{T}}]^{\mathrm{T}}$, $\widehat{\omega} = \boldsymbol{z}_2^\dagger \widehat{\boldsymbol{M}}_{22}^{-1} \boldsymbol{z}_2$, and $\widehat{\lambda}(\varepsilon) = \min\{1 + \varepsilon, \max(1/\widehat{\omega}, 1 - \varepsilon)\}$;
- the optimal solution to the optimization problem in (2) is

$$\widehat{\alpha} = \frac{\boldsymbol{e}_1^\dagger \widehat{\boldsymbol{M}}^{-1} \boldsymbol{z}}{\boldsymbol{e}_1^\dagger \widehat{\boldsymbol{M}}^{-1} \boldsymbol{e}_1}, \tag{5}$$

$$\widehat{\boldsymbol{R}} = \widehat{\boldsymbol{M}}^{\frac{1}{2}} \boldsymbol{U}^\dagger \operatorname{Diag}\left(\frac{1}{\widehat{\lambda}(\varepsilon)}, \frac{1}{1+\varepsilon}, \ldots, \frac{1}{1+\varepsilon}\right) \boldsymbol{U} \widehat{\boldsymbol{M}}^{\frac{1}{2}}, \tag{6}$$

  with $\boldsymbol{U}$ containing the eigenvectors of the following matrix

$$\widehat{\boldsymbol{M}}^{\frac{1}{2}} (\boldsymbol{z} - \widehat{\alpha}\boldsymbol{e}_1)(\boldsymbol{z} - \widehat{\alpha}\boldsymbol{e}_1)^\dagger \widehat{\boldsymbol{M}}^{\frac{1}{2}} = \boldsymbol{U}^\dagger \operatorname{Diag}(\widehat{\omega}, 0, \ldots, 0) \boldsymbol{U}.$$

Note that the tuning parameter ε needs to be set based on the strength of the diffuse multipath returns.

III. Adaptive Selection of Parameter

The performance of the tunable detection statistic $T_{\text{T-AMF}}(\varepsilon)$ depends on the tuning parameter ε. In general, the T-AMF requires an appropriate selection of ε, which is related to the strength of the diffuse multipath echoes. Specifically, for strong reflection contributions, a high value of ε should be used, while for weak multipath signal, an ε value close to zero is reasonable. Unfortunately, prior knowledge of ε is not usually available. As a result, an effective adaptive selection of the tuning parameter is highly valuable in application. This section is devoted to the development of a data-dependent approach to selecting the value of ε.

Before proceeding, it is worth highlighting that the hypothesis testing problem (1) amounts to discriminating between

$$\mathcal{H}_0 : \alpha = 0, \boldsymbol{\Sigma} = \boldsymbol{0} \text{ and } \mathcal{H}_1 : |\alpha| > 0. \tag{7}$$

Moreover, the alternative hypothesis $\mathcal{H}_1$ can be split into two further hypotheses:

$$\mathcal{H}_{10} : |\alpha| > 0, \boldsymbol{\Sigma} = \boldsymbol{0}, \quad \mathcal{H}_{11} : |\alpha| > 0, \|\boldsymbol{\Sigma}\|_2 > 0, \tag{8}$$

which correspond to the multipath-free and multipath-present situations, respectively.

A two-stage procedure is adopted to select a suitable value of ε: i) make a decision for the presence or absence of multipath; ii) estimate the uncertainty size ε when the presence of multipath is established. Details on the joint detection and estimation process are reported below.

A. Detection of The Multipath Effects

The multipath detection problem can be formulated as the following binary hypothesis test:

$$\overline{\mathcal{H}}_0 : \boldsymbol{\Sigma} = \mathbf{0}, \quad \mathcal{H}_{11} : \|\boldsymbol{\Sigma}\|_2 > 0, \tag{9}$$

where $\overline{\mathcal{H}}_0 = \mathcal{H}_0 \bigcup \mathcal{H}_{10}$, and α acts as a nuisance parameter. If the $\overline{\mathcal{H}}_0$ hypothesis is accepted, ε is set to 0 directly; otherwise, an appropriate estimate of ε reflecting the strength of the multipath contributions is proposed.

Note that (9) is equivalent to the one-sided hypothesis testing problem:

$$\overline{\mathcal{H}}_0 : \boldsymbol{R} = \boldsymbol{M}, \quad \mathcal{H}_{11} : \boldsymbol{R} \succeq \boldsymbol{M} \text{ and } \boldsymbol{R} \neq \boldsymbol{M}. \tag{10}$$

For known α and $\boldsymbol{M}$, an ED statistic for (10) in the whitened space after removing the possible target is defined by

$$\left\| \boldsymbol{M}^{-\frac{1}{2}} (\boldsymbol{z} - \alpha \boldsymbol{e}_1)(\boldsymbol{z} - \alpha \boldsymbol{e}_1)^\dagger \boldsymbol{M}^{-\frac{1}{2}} \right\|_2. \tag{11}$$

In fact, resorting to the GLR criterion leads to a test equivalent to the ED in the case (i.e., known α and $\boldsymbol{M}$). Then, a two-step ED for (9) is proposed replacing the unknown α and $\boldsymbol{M}$ in (11) with $\widehat{\alpha}$ and $\widehat{\boldsymbol{M}}$, respectively:

$$\begin{aligned} T_{\text{2S-ED}} &= \left\| \widehat{\boldsymbol{M}}^{-\frac{1}{2}} (\boldsymbol{z} - \widehat{\alpha} \boldsymbol{e}_1)(\boldsymbol{z} - \widehat{\alpha} \boldsymbol{e}_1)^\dagger \widehat{\boldsymbol{M}}^{-\frac{1}{2}} \right\|_2 \\ &= \boldsymbol{z}_2^\dagger \widehat{\boldsymbol{M}}_{22}^{-1} \boldsymbol{z}_2 = \widehat{\omega} \underset{\overline{\mathcal{H}}_0}{\overset{\mathcal{H}_{11}}{\gtrless}} \eta_0, \end{aligned} \tag{12}$$

where η_0 is set to guarantee the desired probability of false alarm P_{f0}.

B. EL-Based Estimation of ε

The EL method that provides an inherently solid way to estimate unknown parameter values, has been deeply studied in [25]–[28]. For our problem, accounting for the unknown α, the likelihood ratio with respect to the primary data covariance matrix $\boldsymbol{R}$ is given by

$$LR(\boldsymbol{R}|\boldsymbol{z}, \alpha) = \frac{(\boldsymbol{z} - \alpha \boldsymbol{e}_1)^\dagger \boldsymbol{R}^{-1} (\boldsymbol{z} - \alpha \boldsymbol{e}_1)}{\exp\left[(\boldsymbol{z} - \alpha \boldsymbol{e}_1)^\dagger \boldsymbol{R}^{-1} (\boldsymbol{z} - \alpha \boldsymbol{e}_1) - 1\right]}. \tag{13}$$

Now, the unknown amplitude α is replaced by its maximum likelihood estimate $\widetilde{\alpha} = \frac{\boldsymbol{e}_1^\dagger \boldsymbol{R}^{-1} \boldsymbol{z}}{\boldsymbol{e}_1^\dagger \boldsymbol{R}^{-1} \boldsymbol{e}_1}$ to remove the dependency of the likelihood ratio on the unknown parameter, leading to

$$\begin{aligned} LR(\boldsymbol{R}|\boldsymbol{z}) &\triangleq LR(\boldsymbol{R}|\boldsymbol{z}, \alpha = \widetilde{\alpha}) \\ &= \frac{(\boldsymbol{z} - \widetilde{\alpha} \boldsymbol{e}_1)^\dagger \boldsymbol{R}^{-1} (\boldsymbol{z} - \widetilde{\alpha} \boldsymbol{e}_1^\dagger)}{\exp\left[(\boldsymbol{z} - \widetilde{\alpha} \boldsymbol{e}_1)^\dagger \boldsymbol{R}^{-1} (\boldsymbol{z} - \widetilde{\alpha} \boldsymbol{e}_1) - 1\right]} && (14) \\ &= \frac{\boldsymbol{z}_2^\dagger \boldsymbol{R}_{22}^{-1} \boldsymbol{z}_2}{\exp\left(\boldsymbol{z}_2^\dagger \boldsymbol{R}_{22}^{-1} \boldsymbol{z}_2 - 1\right)}, && (15) \end{aligned}$$

where $\boldsymbol{R}_{22}$ is the $(N-1) \times (N-1)$ submatrix of $\boldsymbol{R}$ obtained by removing the first row and column from $\boldsymbol{R}$. Since $\boldsymbol{R}_{22}^{-\frac{1}{2}} \boldsymbol{z}_2 \sim \mathcal{CN}_{N-1}(\mathbf{0}, \boldsymbol{I}_{N-1})$, it follows that the expression in (15) is scenario-free (depending only on N), and its pdf, denoted by $p(LR)$, can be precalculated. In fact, by further inspection of (15), $LR(\boldsymbol{R}|\boldsymbol{z})$ gives exactly the likelihood ratio with respect to $\boldsymbol{R}_{22}$ relying on the line-of-sight signal-free components $\boldsymbol{z}_2$ of the primary data.

Next, the scenario-free function (15) is used for the estimation of ε. Plugging (6) into (14) gives

$$LR(\varepsilon|\boldsymbol{z}) \triangleq LR(\widehat{\boldsymbol{R}}(\varepsilon)|\boldsymbol{z}) = \frac{\widehat{\lambda}(\varepsilon)\widehat{\omega}}{\exp\left(\widehat{\lambda}(\varepsilon)\widehat{\omega} - 1\right)}. \tag{16}$$

Inspired by the EL method [25], [26], an EL-based estimate of ε is obtained as

$$\widehat{\varepsilon}_{EL} = \arg\min_{\varepsilon \geq 0} \left| LR(\varepsilon|\boldsymbol{z}) - LR_a \right|^2, \tag{17}$$

where LR_a is a precalculated scalar. Specifically, [25] suggests an upper bound of the random variable LR in (15) to define LR_a, i.e., $\int_0^{LR_a} p(LR) d(LR) = 1 - \delta$, with $0 < \delta \ll 1$. The following proposition lays down the bases to obtain an optimal solution to (17).

Proposition 1: Let $LR_0 = LR(0|\boldsymbol{z}) = \frac{\widehat{\omega}}{\exp(\widehat{\omega} - 1)}$ and $\epsilon_\star = |\frac{1}{\widehat{\omega}} - 1|$. Then we have following results:

(i) $LR(\varepsilon|\boldsymbol{z})$ is a strictly increasing function of ε on $[0, \epsilon_\star]$ and keeps constant on $[\epsilon_\star, +\infty)$;

(ii) if $LR_0 \leq LR_a < 1$, the optimal solution $\widehat{\varepsilon}_{EL}$ to the optimization problem (17) is unique;

(iii) if $0 < LR_a < LR_0$, $\widehat{\varepsilon}_{EL} = 0$ is the optimal solution.

Since the optimal solution $\widehat{\varepsilon}_{EL}$ belongs to the bounded interval $[0, \epsilon_\star]$, the bisection method is an efficient way to solve (17).

C. Automatically T-AMF (AT-AMF)

Combining the T-AMF (3), the two-step ED (12), and the EL-based estimate (17), the Automatically T-AMF (AT-AMF) is defined as

$$T_{\text{AT-AMF}} = T_{\text{T-AMF}}\left[\widehat{\varepsilon}_{EL} \times u(T_{\text{2S-ED}} - \eta_0)\right] \underset{\mathcal{H}_0}{\overset{\mathcal{H}_1}{\gtrless}} \eta, \tag{18}$$

where $u(x)$ is the unit-step function $u(x) = \begin{cases} 1 & x \geq 0 \\ 0 & x < 0 \end{cases}$, and η is the threshold set according to the desired probability of false alarm P_{fa}. The block scheme of the AT-AMF is showed in Fig. 1.

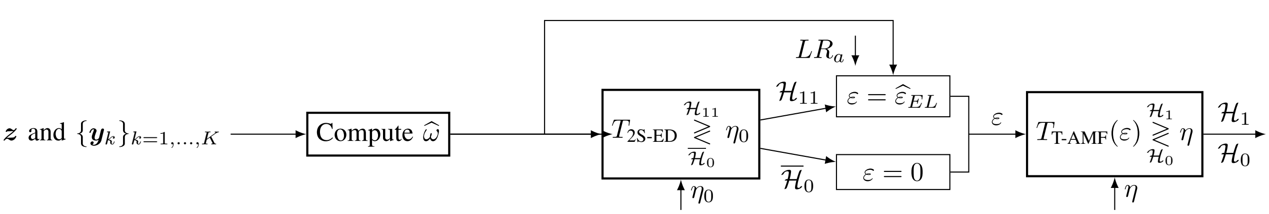

Fig. 1. Block scheme of the AT-AMF test.

It is worth pointing out that the pdf of the AT-AMF under $\mathcal{H}_0$ is independent of the nuisance parameter $\boldsymbol{M}$, and thus it is a CFAR test. To demonstrate it, observe that $T_{\text{AT-AMF}}$ is constructed from $T_{\text{T-AMF}}$, $T_{\text{2S-ED}}$, and $\widehat{\varepsilon}_{EL}$, which are all functions of $T_1 \triangleq \{\boldsymbol{z}^\dagger \widehat{\boldsymbol{M}}^{-1}\boldsymbol{z},\ \boldsymbol{z}_2^\dagger \widehat{\boldsymbol{M}}_{22}^{-1}\boldsymbol{z}_2\}$. It has been proven that the distribution of T_1 under $\mathcal{H}_0$ does not depend on $\boldsymbol{M}$ [18]. As a result, the pdf of $T_{\text{AT-AMF}}$ is parameter-free under the null hypothesis.

IV. Performance Analysis

This section aims at assessing the performance of the devised AT-AMF and the T-AMF with different predetermined ε. Meanwhile, the CAD [22], the AMF [30], and the GLR test [7] are taken for comparison. According to [22], the tuning parameter of the CAD is set to 0.5 in the following case studies. A clairvoyant benchmark is obtained evaluating the GLR test statistic with known disturbance and multipath covariance matrices.

Standard Monte Carlo counting techniques are used to calculate the thresholds and the probabilities of detection for the considered detectors. To limit the computation burden, assume that $P_{fa} = 10^{-3}$ for the target detection, and $P_{f0} = 0.5 \times P_{fa}$ for the two-step ED (12). Then, the thresholds needed to ensure the preassigned P_{fa} and P_{f0} values are evaluated via $100/P_{fa}$ and $100/P_{f0}$ independent trails, respectively. Moreover, the detection probabilities (P_d) are estimated using 5×10^3 independent realizations of the decision rules. The precalculated LR_a is evaluated exploiting 10^6 independent realizations with $\delta = 10^{-2}$.

Assume a spatial processing with $N = 16$ receiving antennas. The nominal line-of-sight steering vector $\boldsymbol{p} = \boldsymbol{v}(0)$ is given by

$$\boldsymbol{v}(\theta) = \frac{1}{\sqrt{N}}\left[1, e^{\jmath 2\pi \frac{d}{\lambda}\sin(\theta)}, \ldots, e^{\jmath 2\pi (N-1)\frac{d}{\lambda}\sin(\theta)}\right]^{\mathrm{T}}, \quad (19)$$

where d is the inter-element spacing, λ is the operating wavelength, and θ is the angle off-boresight of the impinging echoes.

The disturbance covariance matrix is modeled as

$$\overline{\boldsymbol{M}} = \sigma_n^2 \boldsymbol{I}_N + \sigma_c^2 \overline{\boldsymbol{M}}_c, \quad (20)$$

where $\sigma_c^2 > 0$ is the clutter power, $\sigma_n^2 > 0$ is the thermal noise power, and $\overline{\boldsymbol{M}}_c$ is the normalized clutter covariance matrix with the (i, j)-th entry $0.95^{|i-j|}$. Besides, the clutter-to-noise ratio is set to $\sigma_c^2/\sigma_n^2 = 50$ dB with $\sigma_n^2 = 1$. In order to average the detection performance, in each independent trial, the amplitude parameter is simulated according to $\alpha \sim \mathcal{CN}(0, \rho)$, where $\rho \geq 0$ is used to achieve a desired average signal-to-interference-plus-noise ratio (SINR):

$$\text{SINR} \triangleq \mathrm{E}\left[|\alpha|^2\right]\boldsymbol{p}^\dagger \overline{\boldsymbol{M}}^{-1}\boldsymbol{p} = \rho \boldsymbol{p}^\dagger \overline{\boldsymbol{M}}^{-1}\boldsymbol{p}. \quad (21)$$

To describe multipath effects, assume that the glistening surface produces $N_{ML} = 4$ returns impinging on the mainlobe and $N_{SL} = 4$ returns from the sidelobe directions. The covariance matrix of the primary data $\overline{\boldsymbol{z}}$ is modeled as $\overline{\boldsymbol{M}} + \overline{\boldsymbol{\Sigma}}(\alpha, L)$, where the multipath covariance matrix $\overline{\boldsymbol{\Sigma}}(\alpha, L)$ is given by

$$\overline{\boldsymbol{\Sigma}}(\alpha, L) = \sum_{n=1}^{N_{ML}+N_{SL}} \frac{|\alpha|^2}{L}\boldsymbol{v}(\theta_n)\boldsymbol{v}(\theta_n)^\dagger, \quad (22)$$

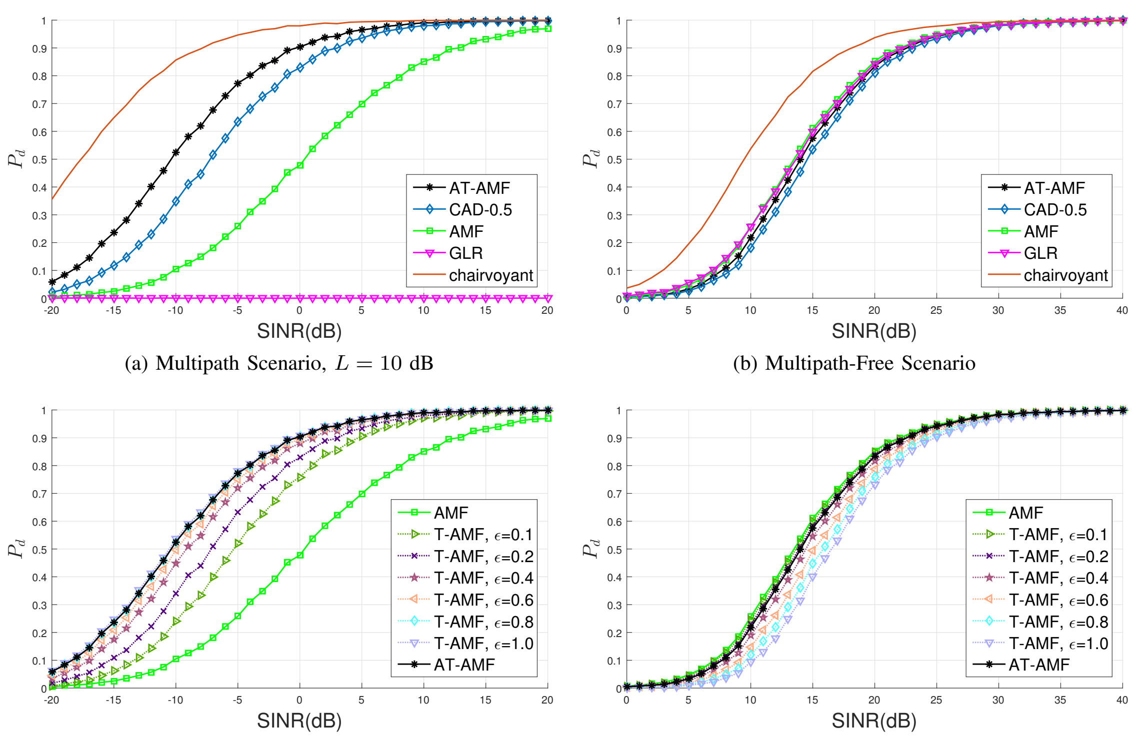

(a) Multipath Scenario, $L = 10$ dB

(b) Multipath-Free Scenario

(c) Multpath Scenario, $L = 10$ dB

(d) Multipath-Free Scenario

Fig. 2. P_d versus SINR for the considered detectors, $K = 32$.

where L is used to adjust the severity of the multipath, for mainlobe scatterers, $\theta_n, n = 1, \ldots, N_{ML}$ are i.i.d. uniform random variables over $[-2, 2]$ degrees, and for the sidelobe scatterers, $\theta_n, n = N_{ML} + 1, \ldots, M_{ML} + N_{SL}$ are i.i.d. uniform random variables over $[8.5, 11.5]$ degrees. Note that $\overline{\mathbf{\Sigma}}$ depends on α (the higher the target reflectivity, the stronger the multipath contributions). Meanwhile, when $L \gg 0$, the multipath-free environment occurs, and when L decreases, the effects of the multipath become more severe.

Fig. 2 displays the P_d of the considered detectors versus SINR for different scenarios, i.e., either $L = 10$ dB (referring to a rich scattering diffuse multipath environment) or a multipath-free environment. Fig. 2(a) highlights that the AT-AMF achieves the best performance in the multipath scenario, and the CAD, the AMF, and the GLR suffer some loss. Such behavior can be attributed to the fact that the CAD receiver does not change the tuning parameter adaptively and the AMF and the GLR ignore the multipath effects. Even if in the multipath-free scenario, the AT-AMF has only a very slight degradation of the detection performance compared to the AMF and the GLR devised under the assumption of multipath absence, as shown in Fig. 2(b). Fig. 2(c) and (d) compare the AT-AMF and the T-AMF with fixed ε values, corroborating the effectiveness of the proposed tuning parameter selection approach.

V. Conclusion

Adaptive target detection in the presence of Gaussian interference and possible diffuse multipath has been considered. The diffuse multipath returns have been modeled as a zero-mean Gaussian random vector with unknown covariance matrix. To handle the resulting hypothesis testing problem, the AT-AMF has been proposed, where the tuning parameter in the T-AMF is set jointly exploiting a two-step ED and an EL-based estimation for the strength of multipath returns. Remarkably, the proposed detection strategy possesses the CFAR property. The numerical results have revealed a robust behavior of the AT-AMF with respect to the actual operating environment, i.e., presence or absence of multipath.

References

[1] M. A. Richards, J. A. Scheer, and W. A. Holm, *Principles of Modern Radar, Volume I: Basic Principles*. Edison, NJ, USA: SciTech, 2010.

[2] R. L. Fante, "Cancellation of specular and diffuse jammer multipath using a hybrid adaptive array," *IEEE Trans. Aerosp. Electron. Syst.*, vol. 27, no. 5, pp. 823–837, 1991.

[3] R. L. Fante and J. A. Torres, "Cancellation of diffuse jammer multipath by an airborne adaptive radar," *IEEE Trans. Aerosp. Electron. Syst.*, vol. 31, no. 2, pp. 805–820, 1995.

[4] A. Aubry, A. De Maio, G. Foglia, and D. Orlando, "Diffuse multipath exploitation for adaptive radar detection." *IEEE Trans. Signal Process.*, vol. 63, no. 5, pp. 1268–1281, 2015.

[5] A. D. Pamela and O. W.David, "Performance analysis of the incoherent and skewness matched filter detectors in multipath environments," *IEEE J. Ocean. Eng.*, vol. 20, no. 1, pp. 80–84, 1995.

[6] K. Gerlach and M. J. Steiner, "Adaptive detection of range distributed targets," *IEEE Trans. Signal Process.*, vol. 47, no. 7, pp. 1844–1851, 1999.

[7] E. Conte, A. De Maio, and G. Ricci, "GLRT-based adaptive detection algorithms for range-spread targets," *IEEE Trans. Signal Process.*, vol. 49, no. 7, pp. 1336–1348, 2001.

[8] D. Ciuonzo, A. D. Maio, and D. Orlando, "A unifying framework for adaptive radar detection in homogeneous plus structured interference—Part II: Detectors design," *IEEE Trans. Signal Process.*, vol. 64, no. 11, pp. 2907–2919, 2016.

[9] M. Tang, Y. Rong, J. Zhou, and X. R. Li, "Invariant adaptive detection of range-spread targets under structured noise covariance," *IEEE Trans. Signal Process.*, vol. 65, no. 12, pp. 3048–3061, 2017.

[10] H. T. Hayvaci, A. De Maio, and D. Erricolo, "Improved detection probability of a radar target in the presence of multipath with prior knowledge of the environment," *IET Radar Sonar Navig.*, vol. 7, no. 1, pp. 36–46, 2013.

[11] U. Kumbul and H. T. Hayvaci, "Knowledge-aided adaptive detection with multipath exploitation radar," in *Proc. Sensor Signal Process. for Defence*, Edinburgh, UK, Sep. 2016, pp. 1–4.

[12] ——, "Multipath exploitation for knowledge-aided adaptive target detection," *IET Radar Sonar Navig.*, vol. 13, no. 6, pp. 863–870, 2019.

[13] S. Bose and A. O. Steinhardt, "Adaptive array detection of uncertain rank one waveforms," *IEEE Trans. Signal Process.*, vol. 44, no. 11, pp. 2801–2809, 1996.

[14] E. J. Kelly and K. M. Forsythe, "Adaptive detection and parameter estimation for multidimensional signal models," Lincoln Lab., MIT, Lexington, MA, USA, Tech. Rep. 848, 1989.

[15] R. S. Raghavan, N. Pulsone, and D. J. McLaughlin, "Performance of the GLRT for adaptive vector subspace detection," *IEEE Trans. Aerosp. Electron. Syst.*, vol. 32, no. 4, pp. 1473–1487, 1996.

[16] S. Kraut, L. L. Scharf, and L. T. McWhorter, "Adaptive subspace detectors," *IEEE Trans. Signal Process.*, vol. 49, no. 1, pp. 1–16, 2001.

[17] W. Liu, W. Xie, J. Liu, and Y. Wang, "Adaptive double subspace signal detection in Gaussian background—Part I: Homogeneous environments," *IEEE Trans. Signal Process.*, vol. 62, no. 9, pp. 2345–2357, 2014.

[18] D. Ciuonzo, A. D. Maio, and D. Orlando, "A unifying framework for adaptive radar detection in homogeneous plus structured interference—Part I: On the maximal invariant statistic," *IEEE Trans. Signal Process.*, vol. 64, no. 11, pp. 2894–2906, 2016.

[19] M. Tang, Y. Rong, A. De Maio, C. Chen, and J. Zhou, "Adaptive radar detection in Gaussian disturbance with structured covariance matrix via invariance theory," *IEEE Trans. Signal Process.*, vol. 67, no. 21, pp. 5671–5685, 2019.

[20] O. Besson, "Adaptive detection with bounded steering vectors mismatch angle," *IEEE Trans. Signal Process.*, vol. 55, no. 4, pp. 1560–1564, 2007.

[21] A. De Maio, S. De Nicola, Y. Huang, S. Zhang, and A. Farina, "Adaptive detection and estimation in the presence of useful signal and interference mismatches," *IEEE Trans. Signal Process.*, vol. 57, no. 2, pp. 436–450, 2009.

[22] F. Bandiera, A. De Maio, and G. Ricci, "Adaptive CFAR radar detection with conic rejection," *IEEE Trans. Signal Process.*, vol. 55, no. 6, pp. 2533–2541, 2007.

[23] F. Bandiera, D. Orlando, and G. Ricci, "CFAR detection strategies for distributed targets under conic constraints," *IEEE Trans. Signal Process.*, vol. 57, no. 9, pp. 3305–3316, 2009.

[24] A. De Maio, "Robust adaptive radar detection in the presence of steering vector mismatches," *IEEE Trans. Aerosp. Electron. Syst.*, vol. 41, no. 4, pp. 1322–1337, 2005.

[25] Y. I. Abramovich, N. K. Spencer, and A. Y. Gorokhov, "Modified GLRT and AMF framework for adaptive detectors," *IEEE Trans. Aerosp. Electron. Syst.*, vol. 43, no. 3, pp. 1017–1051, 2007.

[26] Y. I. Abramovich and B. A. Johnson, "GLRT-based detection-estimation for undersampled training conditions," *IEEE Trans. Signal Process.*, vol. 56, no. 8, pp. 3600–3612, 2008.

[27] O. Besson and Y. I. Abramovich, "Regularized covariance matrix estimation in complex elliptically symmetric distributions using the expected likelihood approach—Part 2: The under-sampled case," *IEEE Trans. Signal Process.*, vol. 61, no. 23, pp. 5819–5829, 2013.

[28] B. Kang, V. Monga, M. Rangaswamy, and Y. Abramovich, "Expected likelihood approach for determining constraints in covariance estimation," *IEEE Trans. Aerosp. Electron. Syst.*, vol. 52, no. 5, pp. 2139–2156, 2016.

[29] Y. Rong, A. Aubry, A. De Maio, and M. Tang, "Diffuse multipath exploitation for adaptive detection of range distributed targets," *IEEE Trans. Signal Process.*, vol. 68, pp. 1197–1212, 2020.

[30] F. C. Robey, D. R. Fuhrmann, E. J. Kelly, and R. Nitzberg, "A CFAR adaptive matched filter detector," *IEEE Trans. Aerosp. Electron. Syst.*, vol. 28, no. 1, pp. 208–216, 1992.